



Contents lists available at SciVerse ScienceDirect

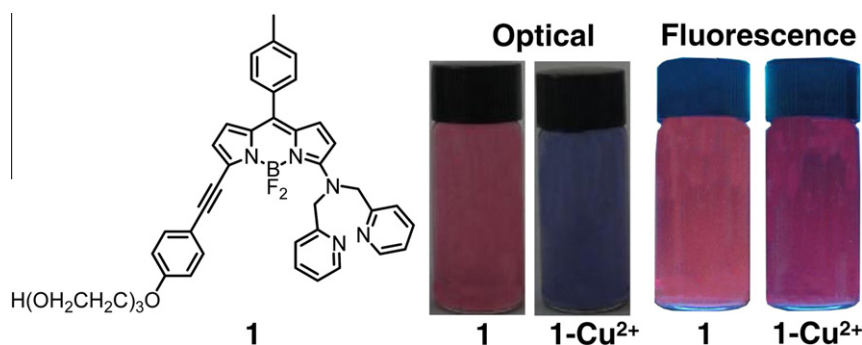
Spectrochimica Acta Part A: Molecular and Biomolecular Spectroscopy

journal homepage: www.elsevier.com/locate/saaA BODIPY derivative as a colorimetric, near-infrared and turn-on chemosensor for Cu²⁺Shouchun Yin^{a,*}, Wenli Yuan^a, Jinlong Huang^a, Danbo Xie^a, Bin Liu^a, Kezhi Jiang^b, Huayu Qiu^a^a College of Material Chemistry and Chemical Engineering, Hangzhou Normal University, Hangzhou 310036, PR China^b Key Laboratory of Organosilicon Chemistry and Material Technology of Ministry of Education, Hangzhou Normal University, Hangzhou, PR China

HIGHLIGHTS

- ▶ A new NIR colorimetric fluorescent chemosensor **1** has been synthesized.
- ▶ **1** Displays a high selectivity for Cu²⁺ with ~250-fold fluorescence enhancement.
- ▶ The distinct color changes also provide **1** as colorimetric sensor for Cu²⁺.

GRAPHICAL ABSTRACT



ARTICLE INFO

Article history:

Received 2 March 2012

Received in revised form 16 April 2012

Accepted 19 April 2012

Available online 9 May 2012

Keywords:

BODIPY

Fluorescent sensor

Copper (II)

Spectroscopic properties

ABSTRACT

A new colorimetric and near-infrared (NIR) fluorescent chemosensor (**1**) for Cu²⁺ based on BODIPY has been synthesized and investigated in this work. **1** Displays a high selectivity for Cu²⁺ with about 250-fold enhancement in fluorescence emission intensity and micromolar sensitivity ($K_d = 2.8 \pm 0.3 \mu\text{M}$) in comparison with alkali and alkaline earth metal ions (Na⁺, K⁺, Mg²⁺, Ca²⁺) and other metal ions (Ba²⁺, Zn²⁺, Cd²⁺, Fe²⁺, Pb²⁺, Ni²⁺, Co²⁺, Ag⁺) upon excitation at 635 nm in CH₃CN. Meanwhile, the distinct color changes and rapid switch-on fluorescence also provide **1** as colorimetric sensor for Cu²⁺.

© 2012 Elsevier B.V. All rights reserved.

1. Introduction

Among the essential transition metal ions in the human body, Cu²⁺ is the third most abundant after Fe³⁺ and Zn²⁺ because it plays an important role in many biological processes as a catalytic cofactor for a variety of metalloenzymes, including tyrosinase, superoxide dismutase and cytochrome oxidase [1,2]. Meanwhile, Cu²⁺ is high toxic to some organisms. If unregulated, Cu²⁺ can lead to the disturbance of the cellular homeostasis, causing oxidative stress and disorders associated with neurodegenerative diseases,

such as Menkes disease, Wilson disease, and Alzheimer disease [3]. Thus, the determination of copper is important due to its utility as well as toxicity. Most of the reported Cu²⁺ ions fluorescent chemosensors work in a turn-off mode due to the quenching effect of paramagnetic nature of Cu²⁺ [4–20]. For the practical applications, fluoroionophores showing turn-on (fluorescence enhancement) as a result of metal-ion binding are more interesting. Although Cu²⁺ fluorescence turn-on mode sensors are steadily increasing [21–31], however, there are a few reports about near-infrared (NIR) or red fluorescent turn-on sensor for Cu²⁺ [32–34]. Fluorescence probes for NIR or red detection are preferable for applications in biological systems because they can reduce autofluorescence and photodamage to living cells [35]. Thus, there is

* Corresponding author. Tel./fax: +86 571 28867899.

E-mail address: yinsc@ustc.edu (S. Yin).

still strong demand for new Cu²⁺ sensors, especially that can be excited in NIR or red region.

In recent year, 4,4-difluoro-4-bora-3a,4a-diaza-s-indacenes (abbreviated as BODIPYs) have gained a great deal of attention due to their outstanding properties, such as large molar absorption coefficients, narrow absorption and emission bands located in the visible region, high fluorescence quantum yields and excellent stability. Moreover, their spectroscopic and photophysical properties can be fine-tuned by structural modification at the appropriate positions of the difluoroboron dipyrromethene core. The attachment of aryl group at the 2,3,5,6 positions of the difluoroboron dipyrromethene core can greatly red-shift the absorption and emission bands of BODIPY dyes to NIR or red region [36–38].

Herein, we report the synthesis and metal ion recognition properties of a new BODIPY based sensor, 5-*N*-(2-picolyl)amine-4,4-difluoro-3-(4-(hydroxy(ethyloxy(ethyloxy(ethyloxy)))) phenylethynyl)-8-(4-tolyl)-4-bora-3a,4a-diaza-s-indacene (**1**). **1** displays a high selectivity for Cu²⁺ with about 250-fold enhancement in fluorescence emission intensity in comparison with all other test metal ions upon excitation at red region ($\lambda_{\text{ex}} = 635 \text{ nm}$) in CH₃CN.

2. Experimental

2.1. Apparatus

¹H and ¹³C NMR spectra were recorded at room temperature on a Bruker Avance 400 operating at a frequency of 400 MHz for ¹H and 100 MHz for ¹³C. Melting points were taken on a Beijing Taike X-5 melting point instrument and are uncorrected. Mass spectra were recorded on a Hewlett–Packard 5989 A mass spectrometer (ESI mode). High-resolution mass data were obtained with a Kratos MS50TC instrument. UV–Vis absorption spectra were recorded on a Perkin Elmer Lambda 40 UV–Vis spectrophotometer. Corrected steady-state excitation and emission spectra were obtained using a HITACHI F-2700 Fluorescence Spectrophotometer.

2.2. Reagents

3,5-Dichloro-8-(4-tolyl)BODIPY [39] and 2-(2-(2-(4-ethynylphenoxy)ethoxy)ethoxy)ethanol [40] was synthesized according to literature procedures. Other reagents were purchased from Acros and used without further purification.

2.3. Determination of ground-state dissociation constant K_d

The ground-state dissociation constant K_d of the complex between **1** and Cu²⁺ was determined in CH₃CN solution at 25 °C by direct fluorometric titration as a function of Cu²⁺ using the fluorescence emission spectra. Nonlinear fitting of Eq. (1) to the steady-state fluorescence data F recorded as a function of [Cu²⁺] yields values of K_d , F_{min} , F_{max} , and n .

$$F = \frac{F_{\text{max}}[\text{Cu}^{2+}]^n + F_{\text{min}}K_d}{K_d + [\text{Cu}^{2+}]^n} \quad (1)$$

In Eq. (1), F stands for the fluorescence signal at [Cu²⁺], whereas F_{min} and F_{max} denote the fluorescence signals at minimal and maximal [Cu²⁺], respectively, and n is the number of Cu²⁺ ions bound per probe molecule (i.e., stoichiometry of binding) [41].

2.4. Synthesis of 5-Chloro-4,4-difluoro-3-(4-(hydroxy(ethyloxy(ethyloxy(ethyloxy))))phenylethynyl)-8-(4-tolyl)-4-bora-3a,4a-diaza-s-indacene (**2**)

315 mg (0.9 mmol) 3,5-dichloro-8-(4-tolyl) BODIPY and 75 mg (0.3 mmol) 2-(2-(2-(4-ethynylphenoxy)ethoxy)ethoxy)ethanol (**3**)

were dissolved in 15 mL of THF and 50 μL of Et₃N under argon. To this solution 14 mg (0.02 mmol) PdCl₂(PPh₃)₂ and 4 mg (0.02 mmol) CuI were added. The reaction mixture was heated at 60 °C for 12 h. After evaporating the solvent, the crude product was extracted with CH₂Cl₂ (3 \times 40 mL), dried over MgSO₄, and the solvent was evaporated under reduced pressure. Purification was performed by chromatography on silica gel with CH₂Cl₂/acetone (15:1, v/v) as eluent to give purple solid **2** (147 mg, 87% yield). ¹H NMR (400 MHz, CDCl₃) δ (ppm): 7.61 (2H, d, $J = 8.8 \text{ Hz}$), 7.41 (2H, t, $J = 8.0 \text{ Hz}$), 7.32 (2H, d), 6.93 (2H, d), 6.78 (1H, d, $J = 4.4 \text{ Hz}$), 6.85 (1H, d), 6.69 (1H, d, $J = 4.2 \text{ Hz}$), 6.42 (1H, d), 4.18 (2H, t, $J = 4.6 \text{ Hz}$), 3.89 (2H, t, $J = 4.4 \text{ Hz}$), 3.73 (6H, m), 3.63 (2H, t, $J = 4.0 \text{ Hz}$, OH), 2.47 (3H, s, Ar-CH₃).

2.5. Synthesis of 5-*N*-(2-picolyl)amine-4,4-difluoro-3-(4-(hydroxy(ethyloxy(ethyloxy(ethyloxy)))) phenylethynyl)-8-(4-tolyl)-4-bora-3a,4a-diaza-s-indacene (**1**)

To a solution of **2** (113 mg, 0.2 mmol) and di(2-picolyl)amine (20 mg, 0.2 mmol) in 20 mL of acetonitrile, sodium hydride (5 mg, 0.2 mmol) was added. The reaction mixture was stirred at room temperature for 12 h under argon. After evaporating the solvent, 20 mL of water was added and the organic layer was extracted with CH₂Cl₂ (3 \times 20 mL), dried by MgSO₄, and evaporated under reduced pressure. The crude product was purified by column chromatography on silica gel, eluting with a mixture of CH₂Cl₂/methanol (20:1, v/v) as eluent to give purple solid **1** (83 mg, 57% yield). M.P. 178–179 °C. ¹H NMR (400 MHz, CDCl₃) δ (ppm): 8.55 (2H, d, $J = 3.6 \text{ Hz}$), 7.41 (2H, d, $J = 6.8 \text{ Hz}$), 7.34 (2H, d, $J = 6.4 \text{ Hz}$), 7.22 (4H, m), 6.84 (2H, d, $J = 6.8 \text{ Hz}$), 6.81 (1H, d, $J = 4.0 \text{ Hz}$), 6.55 (1H, d, $J = 3.2 \text{ Hz}$), 6.26 (1H, d), 5.28 (4H, s), 4.14 (2H, t, $J = 5.4 \text{ Hz}$), 3.86 (2H, t, $J = 3.8 \text{ Hz}$), 3.62 (2H, t, $J = 3.6 \text{ Hz}$), 3.71 (6H, m), 3.38 (1H, t, $J = 5.6 \text{ Hz}$, OH), 2.42 (3H, s, Ar-CH₃). ESI–MS: m/z 750.3 [M+Na]⁺. HRMS (MH⁺): calcd. for C₄₂H₄₁BF₂N₅O₄ 728.3220, found 728.3210.

3. Results and discussion

3.1. Synthesis

1 was readily synthesized in two steps from 3,5-dichloroBODIPY as starting material. As outlined in Scheme 1, one chlorine atom of 3,5-dichloroBODIPY was first reacted with **3** by palladium-catalyzed reaction to afford the monosubstituted product **2** in good (87%) yield. Here, the feed ratio of 3,5-dichloroBODIPY and **3** was 3:1 to make sure that **3** can be reacted completely, so that the separation of the desired product was easy. After being purified by chromatography several times, the purity of **2** was enough for NMR spectroscopic characterization. Unlike the reaction of 3,5-dichloroBODIPY with phenylacetylene reported by Wim [42], in this Sonogashira reaction no disubstituted side-product could be found because of the lower reactivity of the second chlorine resulting from the electron donating effect of the oxygen atom. The second chlorine atom of the isolated **2** was then substituted by di(2-picolyl)amine in room temperature with sodium hydride as base to get **1** in modest (57%) yield.

3.2. Spectral characteristics

After full characterization of the chemical structure by NMR and MS spectroscopy, the photophysical properties of **1** upon addition of several metal cations (Na⁺, K⁺, Mg²⁺, Ca²⁺, Ba²⁺, Cu²⁺, Zn²⁺, Cd²⁺, Fe²⁺, Pb²⁺, Ni²⁺, Co²⁺, Ag⁺) in CH₃CN were investigated by UV–Vis absorption and fluorescence spectroscopic measurements and titration studies. Fig. 1 showed the UV–Vis absorption spectra

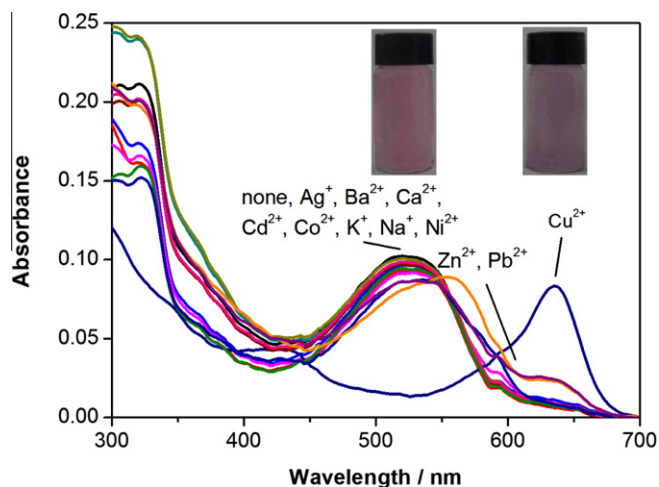
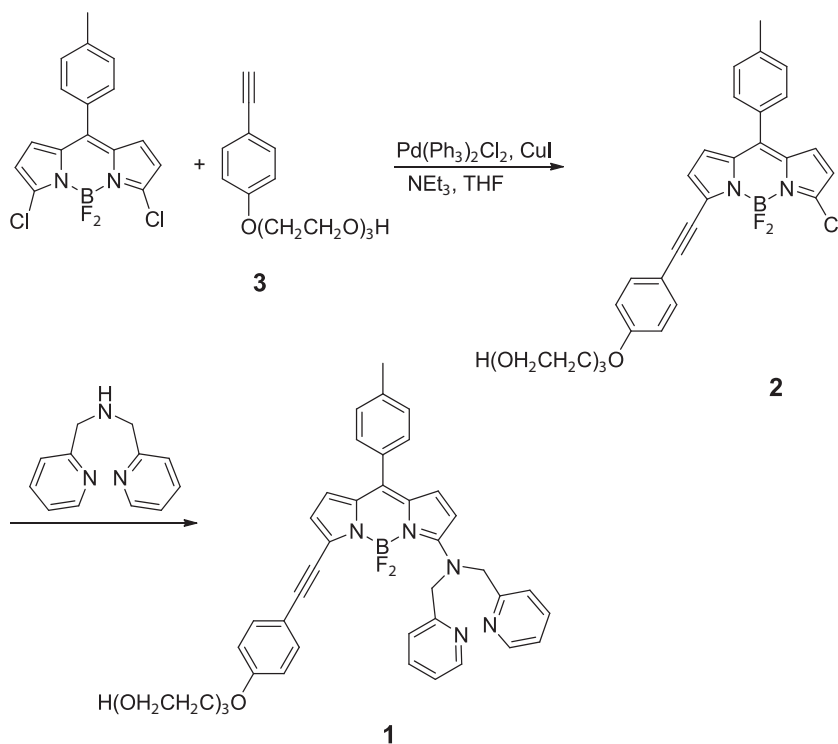


Fig. 1. UV-Vis absorption spectra of **1** in CH_3CN upon addition of various metal ions. The concentration of **1** was $2 \mu\text{M}$ and that of the selected metal ion was $50 \mu\text{M}$.

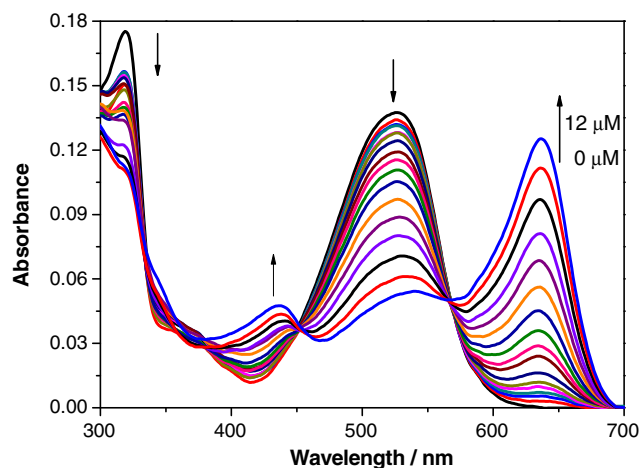


Fig. 2. UV-Vis absorption spectra of **1** ($2 \mu\text{M}$) in the presence of different concentrations of Cu^{2+} (0, 0.125, 0.25, 0.375, 0.5, 0.75, 1, 1.25, 1.5, 2, 2.5, 3, 4, 6, 8, 10, $12 \mu\text{M}$) in CH_3CN .

of **1** with excess amount of the different test metal ions in CH_3CN . When Na^+ , K^+ , Mg^{2+} , Ca^{2+} , Ba^{2+} , Cd^{2+} , Fe^{2+} , Ni^{2+} , Co^{2+} , Ag^+ were added to the CH_3CN solution of **1**, respectively, the UV-Vis absorption spectrum had almost no change and exhibited a main peak at 525 nm assigned to the $S_0 \rightarrow S_1$ transition of the BODIPY chromophore. Zn^{2+} and Pb^{2+} resulted in a new, weak and red absorption band. However, when Cu^{2+} was added, a new, strong and red absorption peak at 636 nm appeared and the main peak at 525 nm disappeared. Fig. 2 showed the UV-Vis absorption titration of **1** with the different Cu^{2+} concentrations in CH_3CN . As shown as in Fig. 2, with the increase of the concentration of Cu^{2+} ions, the

intensity of the main absorption peak at 525 nm decreased gradually and red-shifted to 536 nm, while the intensity of a new band at 636 nm increased continuously. The disappearance of the absorption peak at 525 nm and the appearance of a new peak at 636 nm upon addition of Cu^{2+} resulted in a naked eye color change from pink to purple. The color of **1** in CH_3CN with Zn^{2+} or Pb^{2+} had almost no changes although Zn^{2+} or Pb^{2+} could result in a new, weak, red absorption band (as shown in lower row of Fig. 3). Those results indicated that **1** can be used as a colorimetric probe for Cu^{2+} . The presence of three well-defined isosbestic points at

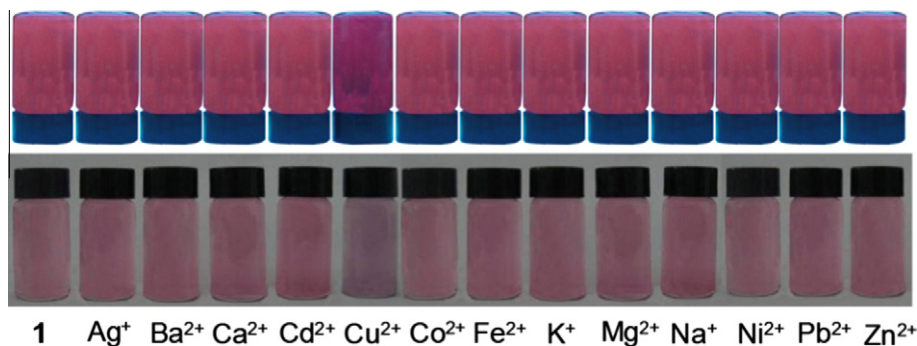


Fig. 3. Photographs of solutions of **1** in CH_3CN upon addition of various metal ions. The concentration of **1** was $2 \mu\text{M}$ and that of the selected metal ion was $50 \mu\text{M}$. Upper row: fluorescence observed upon excitation at 365 nm . Lower row: optical.

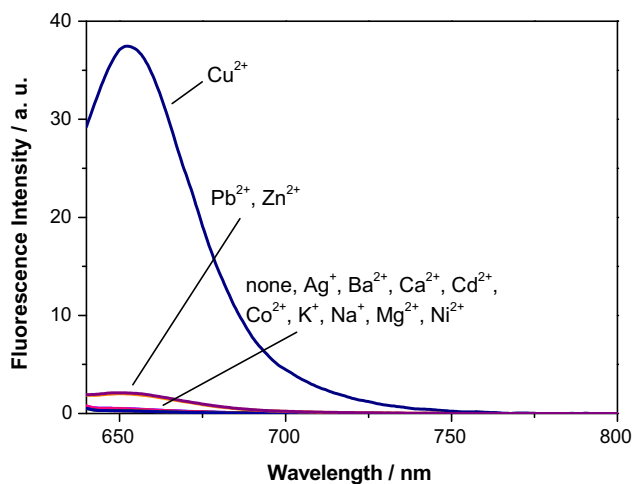


Fig. 4. Fluorescence emission spectra of **1** ($2 \mu\text{M}$) upon addition of various metal ions ($50 \mu\text{M}$) in CH_3CN ($\lambda_{\text{ex}} = 635 \text{ nm}$).

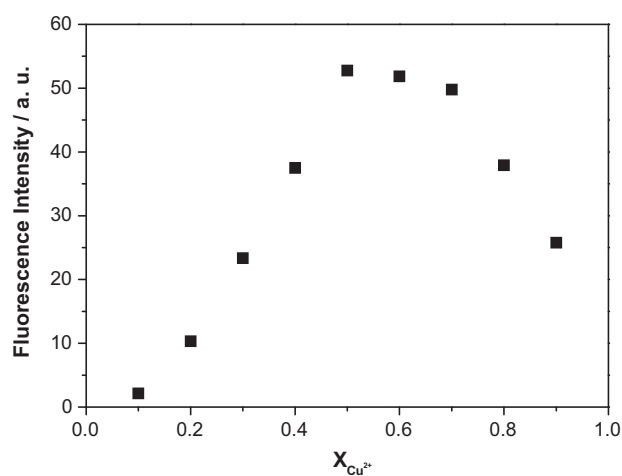


Fig. 6. Job's plot for **1** and Cu^{2+} . The total concentration of **1** and Cu^{2+} was kept at a fixed $4 \mu\text{M}$. The fluorescence intensity was measured at 652 nm .

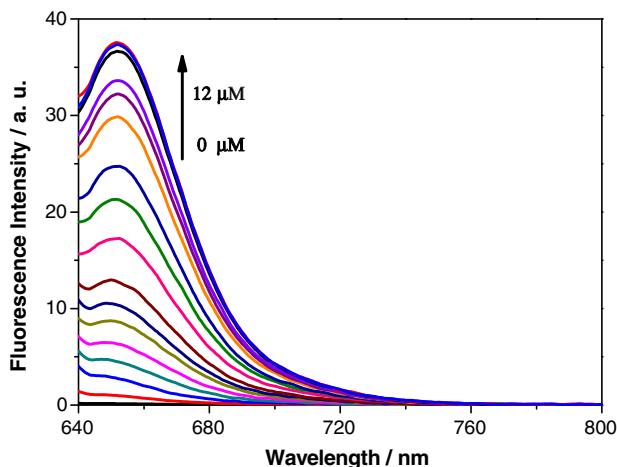


Fig. 5. Fluorescent emission spectra of **1** ($2 \mu\text{M}$) upon excitation at 635 nm in the presence of different concentrations of Cu^{2+} ($0, 0.125, 0.25, 0.375, 0.5, 0.75, 1, 1.25, 1.5, 2, 2.5, 3, 4, 6, 8, 10, 12 \mu\text{M}$) in CH_3CN .

$\lambda = 335, 453$ and 567 nm demonstrated the presence of an equilibrium process corresponding to apo **1** and copper complex **1**- Cu^{2+} . Further addition of excess Cu^{2+} produces no significant change in UV-Vis spectra when the concentration of Cu^{2+} reached $12 \mu\text{M}$.

Since a new, strong and red absorption peak can be produced when Cu^{2+} was added to **1** in CH_3CN , we wondered if Cu^{2+} can

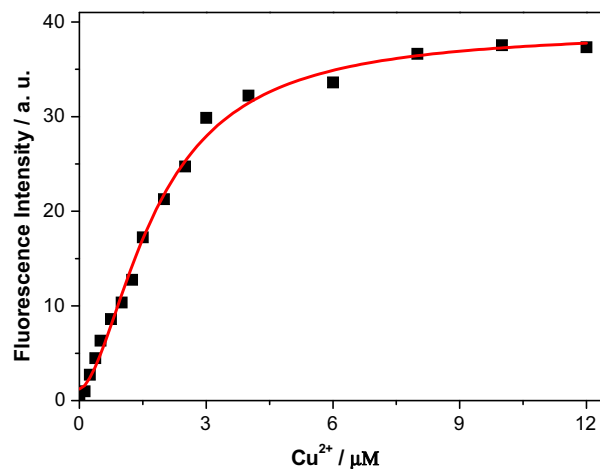
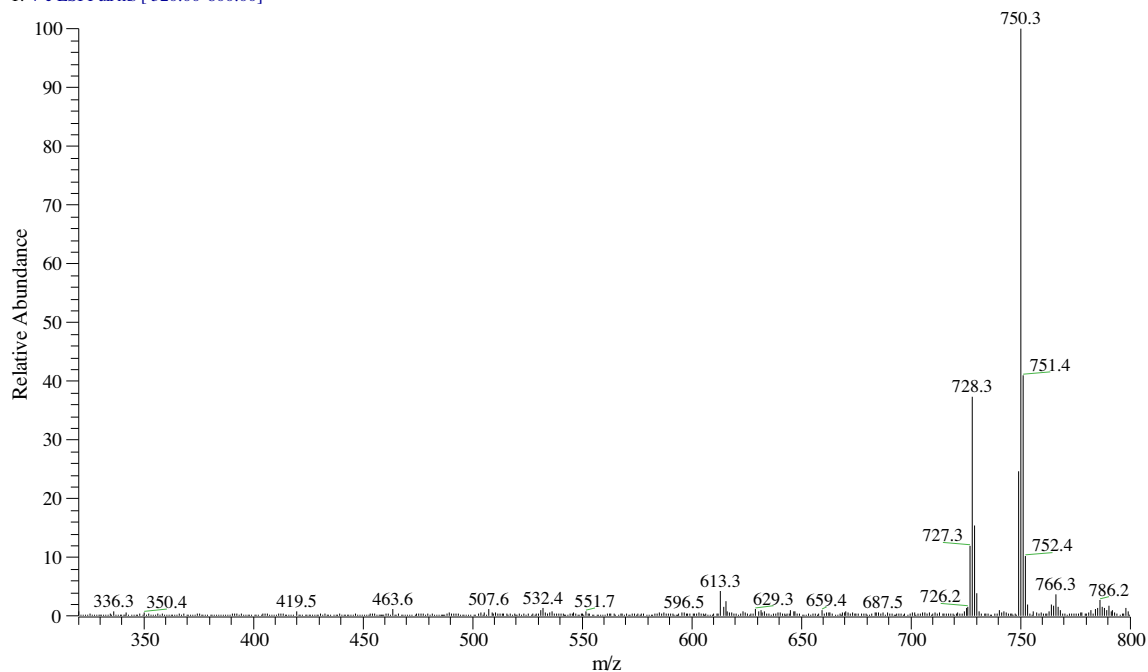


Fig. 7. Fluorescence emission intensity of **1** ($2 \mu\text{M}$) in CH_3CN monitored at 652 nm as a function of Cu^{2+} concentration ($\lambda_{\text{ex}} = 635 \text{ nm}$). The red line represents the best fit to the data (filled squares) according to Eq. (1). (For interpretation of the references to colour in this figure legend, the reader is referred to the web version of this article.)

induce a new red emission when excitation at the maximum absorption of **1**- Cu^{2+} . Fig. 4 displayed the fluorescence emission spectra of **1** ($2 \mu\text{M}$) with the above mentioned metal cations (25

ESI-yinshouchun111013-yin5_01 #4-8 RT: 0.04-0.08 AV: 5 NL: 3.33E7
T: + c ESI Full ms [320.00-800.00]



ESI-yinshouchun111013-yin5-Cu_01 #141-173 RT: 2.33-2.86 AV: 33 NL: 4.58E7
T: + c ESI Full ms [155.00-1200.00]

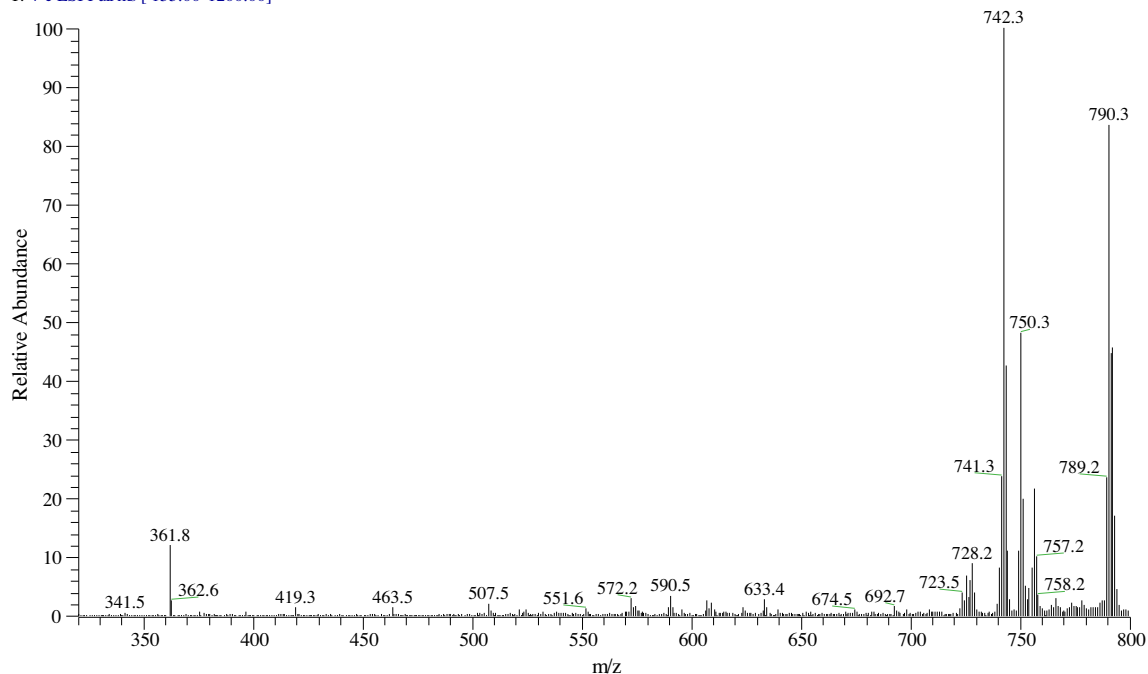


Fig. 8. ESI ms spectra of **1** (top) and **1**-Cu²⁺ (low).

equiv) measured in CH₃CN upon excitation at $\lambda_{\text{ex}} = 635$ nm. As shown in Fig. 4, **1** emitted almost no fluorescence upon excitation at 635 nm because **1** had almost no absorbance at this wavelength. However, when Cu²⁺ ions were added to **1** in CH₃CN, a new strong fluorescence emission with maximum at 652 nm appeared. Under the same conditions, no obvious fluorescence changes were observed for other tested metal ions including Zn²⁺ and Pb²⁺, which only induced negligible fluorescence enhancement at red range compared with Cu²⁺. Those observations indicated that **1** has a very high selectivity for Cu²⁺. We have also investigated the effect of water content on the fluorescence measurement of **1**-Cu²⁺. It has

been found that the fluorescence signal of **1**-Cu²⁺ had already quenched if the water content exceeded 10%. Thus, we will focus our investigation on the metal ion sensing properties of **1** in pure CH₃CN in the following discussion.

To investigate the sensitivity of **1** for Cu²⁺, the fluorescence titration of **1** in the presence of different Cu²⁺ concentrations was then performed. As shown in Fig. 5, upon excited at 635 nm, with the increase of the concentration of Cu²⁺ the fluorescence intensity increased continuously from the background level of free **1**. When the concentration of Cu²⁺ increased to 12 μM , the fluorescence enhancement reached the maximum value (about 250-fold

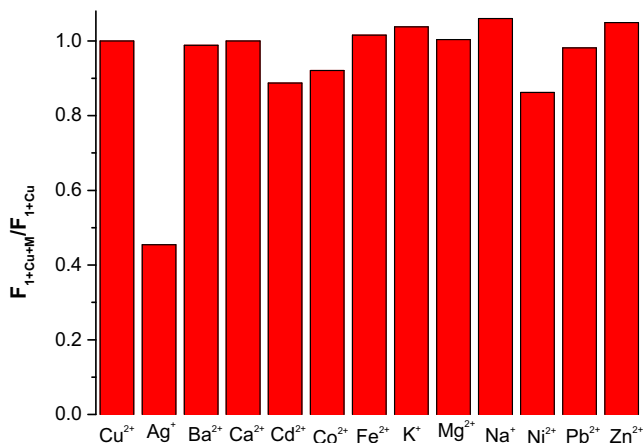


Fig. 9. Fluorescence response of **1** (2 μ M) containing 12 μ M Cu²⁺ to the selected metal ions (50 μ M). F_{1+Cu} and F_{1+Cu+M} denote the fluorescence signals of **1** in the presence of Cu²⁺ only and in the presence of Cu²⁺ as well as the competing ion, respectively. Excitation was at 635 nm and emission was at 652 nm.

enhancement) and the fluorescence quantum yield increased to 0.22 for **1**-Cu²⁺, correspondingly, which indicated that **1** exhibits a very high sensitivity for Cu²⁺.

3.3. Binding stoichiometry of **1** and Cu²⁺

To determine the binding stoichiometry of **1** and Cu²⁺, Job's method for the emission was employed. The total concentration of **1** and Cu²⁺ was kept at a constant 4 μ M, with a continuous variable the molar fraction of Cu²⁺. The change of the fluorescence intensity at 652 nm with the concentration ratio of **1** to Cu²⁺ was shown in Fig. 6. When the molar fraction of Cu²⁺ was about 0.5, the complex of **1** and Cu²⁺ exhibited a maximum fluorescence emission, which indicated that a 1:1 stoichiometry is most possible for the binding mode of **1** and Cu²⁺.

Further evidences for proving a 1:1 stoichiometry for the **1**-Cu²⁺ complex were the result of the nonlinear fitting of the fluorometric titration and ESI mass. Fig. 7 showed the dependence of the emission intensity at 652 nm on the concentration of Cu²⁺ getting the data from Fig. 2. By the nonlinear fitting of the fluorometric titration data using Eq. (1), the stoichiometry of the complex of **1** and Cu²⁺ was obtained as 1:1 and the dissociation constant (K_d) was 2.8 ± 0.3 μ M. The ESI mass spectrum of **1** showed two peaks at $m/z = 728.3$ and 750.3 corresponding to $[1+H]^+$ and $[1+Na]^+$, respectively (seen in Fig. 8), while the complex of **1** and Cu²⁺ exhibited a unique peak at $m/z = 790.3$ corresponding to $[1+Cu-H]^+$, which reveals a 1:1 stoichiometry for the **1**-Cu²⁺ complex.

3.4. Selectivity and tolerance of **1** to Cu²⁺ over other metal ions

To explore the use of **1** as an ion-selective fluorescent probe for Cu²⁺, fluorescent spectra of **1** response to other metal ions (Na⁺, K⁺, Mg²⁺, Ca²⁺, Ba²⁺, Zn²⁺, Cd²⁺, Fe²⁺, Pb²⁺, Ni²⁺, Co²⁺, Ag⁺) that probably affect the fluorescence intensity were also examined. An excess amount of above mentioned metal ions (50 μ M) were added to 12 μ M Cu²⁺ in CH₃CN and the fluorescence response at 652 nm (I_{652}) of **1** was detected and then compared with that of **1** in CH₃CN containing only 12 μ M Cu²⁺. As shown in Fig. 9, the competing metal ions exhibited only a small or no interference with the detection of Cu²⁺ ions except for Ag⁺, which partly quenched the fluorescence of **1**-Cu²⁺. These experimental results showed that without Ag⁺ the response of **1** to Cu²⁺ was unaffected by the presence of the other possible contaminating metal ions, even whose concentration existed 5 times higher than that of Cu²⁺. Therefore, the Cu²⁺-selective

binding and turn-on response could take place in the coexistence of the competitive metal ions in the absence of Ag⁺.

4. Conclusions

In conclusion, we have reported a colorimetric, NIR and turn-on fluorescent sensor **1** based on BODIPY that can sensitively and selectively detect Cu²⁺ in CH₃CN. **1** displays a new strong red absorption peak and a significant fluorescence enhancement in the presence of Cu²⁺ using a red excitation wavelength ($\lambda_{ex} = 635$ nm) in CH₃CN. The obvious changes in the color and fluorescence induced by Cu²⁺ make **1** be as colorimetric sensor. The mechanism of signal change in absorption and emission when Cu²⁺ is bound are not known at this moment and this will be the subject of further study. An answer will hopefully be given in a forthcoming paper.

Acknowledgements

We thank National Natural Science Foundation of China (Nos. 91127032, 21174035), Zhejiang Provincial Natural Science Foundation of China (No. Y4100287), Program for Excellent Young Teachers in Hangzhou Normal University (No. HNUEYT 2011-01-019), and the Opening Foundation of Zhejiang Provincial Top Key Discipline (No. 20110943) for financial supports.

References

- [1] E. Gaggelli, H. Kozłowski, D. Valensin, G. Valensin, Chem. Rev. 106 (2006) 1995–2044.
- [2] E.L. Que, D.W. Domaille, C.J. Chang, Chem. Rev. 108 (2008) 1517–1549.
- [3] K.J. Barnham, C.L. Masters, A.I. Bush, Nat. Rev. Drug Discovery 3 (2004) 205–214.
- [4] S.H. Kim, J.S. Kim, S.M. Park, S.K. Chang, Org. Lett. 8 (2006) 371–374.
- [5] J. Xie, M. Ménand, S. Maisonneuve, R. Métivier, J. Org. Chem. 72 (2007) 5980–5985.
- [6] Z.T. Jiang, R.R. Deng, L. Tang, P. Lu, Sens. Actuators, B 135 (2008) 128–132.
- [7] H.S. Jung, P.S. Kwon, J.W. Lee, J.I. Kim, C.S. Hong, J.W. Kim, S.H. Yan, J.Y. Lee, J.H. Lee, T.H. Joo, J.S. Kim, J. Am. Chem. Soc. 131 (2009) 2008–2012.
- [8] W.B. Chen, X.J. Tu, X.Q. Guo, Chem. Commun. (2009) 1736–1738.
- [9] J.H. Jung, M.H. Lee, H.J. Kim, H.S. Jung, S.Y. Lee, N.R. Shin, K. No, J.S. Kim, Tetrahedron Lett. 50 (2009) 2013–2016.
- [10] M.M. Zhang, K.L. Zhu, F.H. Huang, Chem. Commun. 46 (2010) 8131–8141.
- [11] Z.Q. Guo, W.H. Zhu, H. Tian, Macromolecules 43 (2010) 739–744.
- [12] S.C. Wang, G.W. Men, L.Y. Zhao, Q.F. Hou, S.M. Jiang, Sens. Actuators, B 145 (2010) 826–831.
- [13] M.Q. Zhu, Z. Gu, R. Zhang, J.N. Xiang, S.M. Nie, Talanta 81 (2010) 678–683.
- [14] D. Maity, A.K. Manna, D. Karthigeyan, T.K. Kundu, S.K. Pati, T. Govindaraju, Chem. Eur. J. 17 (2011) 11152–11161.
- [15] L. Zhang, X.D. Lou, Y. Yu, J.G. Qin, Z. Li, Macromolecules 44 (2011) 5186–5193.
- [16] R. Pandey, P. Kumar, A.K. Singh, M. Shahid, P.Z. Li, S.K. Singh, Q. Xu, A. Misra, D.S. Pandey, Inorg. Chem. 50 (2011) 3189–3197.
- [17] X.J. Xie, Y. Qin, Sens. Actuators, B 156 (2011) 213–217.
- [18] A. Helal, M.H.O. Rashid, C.H. Choi, H.S. Kim, Tetrahedron 67 (2011) 2794–2802.
- [19] Y.J. Zhang, X.P. He, M. Hu, Z. Li, X.X. Shi, G.R. Chen, Dyes Pigm. 88 (2011) 391–395.
- [20] G.C. Yu, Z.B. Zhang, C.Y. Han, M. Xue, Q.Z. Zhou, F.H. Huang, Chem. Commun. 48 (2012) 2958–2960.
- [21] Z.C. Wen, R. Yang, H. He, Y.B. Jiang, Chem. Commun. (2006) 106–108.
- [22] X. Qi, E.J. Jun, L. Xu, S.J. Kim, J.S.J. Hong, Y.J. Yoon, J.Y. Yoon, J. Org. Chem. 71 (2006) 2881–2884.
- [23] Y. Xiang, A.J. Tong, Y. Ju, Org. Lett. 8 (2006) 2863–2866.
- [24] G.K. Li, Z.X. Xu, C.F. Chen, Z.T. Huang, Chem. Commun. (2008) 1774–1776.
- [25] M.X. Yu, M. Shi, Z.G. Chen, F.Y. Li, X.X. Li, Y.H. Gao, J. Xu, H. Yang, Z.G. Zhou, T. Yi, C.H. Huang, Chem. Eur. J. 14 (2008) 6892–6900.
- [26] E.L. Que, E. Gianolio, S.L. Baker, A.P. Wong, S. Aime, C.J. Chang, J. Am. Chem. Soc. 131 (2009) 8527–8536.
- [27] Y. Zhao, X.B. Zhang, Z.X. Han, L. Qiao, C.Y. Li, L.X. Jian, G.L. Shen, R.Q. Yu, Anal. Chem. 81 (2009) 7022–7030.
- [28] A. Senthilvelan, I.T. Ho, K.C. Chang, G.H. Lee, Y.H. Liu, W.S. Chung, Chem. Eur. J. 15 (2009) 6152–6160.
- [29] J.F. Zhang, Y. Zhou, J.Y. Yoon, Y. Kim, S.J. Kim, J.S. Kim, Org. Lett. 12 (2010) 3852–3855.
- [30] Z.Q. Hua, X.M. Wang, Y.C. Feng, L. Ding, H.Y. Lu, Dyes Pigm. 88 (2011) 257–261.
- [31] F.A. Abebe, E. Sinn, Tetrahedron Lett. 52 (2011) 5234–5237.
- [32] S.C. Yin, V. Leen, S. Van Snick, N. Boens, W. Dehaen, Chem. Commun. 46 (2010) 6329–6331.

- [33] S. Goswami, D. Sen, N.K. Das, *Org. Lett.* 12 (2010) 856–859.
- [34] S. Goswami, D. Sen, N.K. Das, G. Hazra, *Tetrahedron Lett.* 51 (2010) 5563–5566.
- [35] B.A. Smith, W.J. Akers, W.M. Leevy, A.J. Lampkins, S.Z. Xiao, W. Wolter, M.A. Suckow, S. Achilefu, B.D. Smith, *J. Am. Chem. Soc.* 132 (2010) 67–69.
- [36] A. Loudet, K. Burgess, *Chem. Rev.* 107 (2007) 4891–4932.
- [37] G. Ulrich, R. Ziessel, A. Harriman, *Angew. Chem. Int. Ed.* 47 (2008) 1184–1201.
- [38] V. Leen, N. Boens, W. Dehaen, *Chem. Soc. Rev.* 41 (2012) 1130–1172.
- [39] T. Rohand, M. Baruah, W.W. Qin, N. Boens, W. Dehaen, *Chem. Commun.* (2006) 266–268.
- [40] J.W. Chen, K.L. Cheuk, B.Z. Tang, *J. Polym. Sci. Part A* 44 (2006) 1153–1167.
- [41] W.W. Qin, T. Rohand, W. Dehaen, J.N. Clifford, K. Driesen, D. Beljonne, B. Van Averbeke, M. Van der Auweraer, N. Boens, *J. Phys. Chem. A* 111 (2007) 8588–8597.
- [42] T. Rohand, W.W. Qin, N. Boens, W. Dehaen, *Eur. J. Org. Chem.* (2006) 4658–4663.